

## Modeling AC losses in the ITER NbTi poloidal field full size joint sample (PF-FSJS) using the THELMA code

R. Zanino<sup>a,\*</sup>, M. Bagnasco<sup>a</sup>, F. Bellina<sup>b</sup>, P. Gislon<sup>c</sup>,  
P.L. Ribani<sup>d</sup>, L. Savoldi Richard<sup>a</sup>

<sup>a</sup> *Dipartimento di Energetica, Politecnico, Torino, Italy*

<sup>b</sup> *Dipartimento di Ingegneria Elettrica, Gestionale e Meccanica, Università di Udine, Italy*

<sup>c</sup> *ENEA, Frascati, Italy*

<sup>d</sup> *Dipartimento di Ingegneria Elettrica, Università di Bologna, Italy*

Available online 2 August 2005

### Abstract

A first validation of the full version of the thermal–hydraulic electromagnetic (THELMA) code, developed for the analysis of transients in the cable-in-conduit conductors and coils relevant for the International Thermonuclear Experimental Reactor (ITER) is presented here. THELMA includes electromagnetic models of the cable joints and terminations (lumped parameter) and of the conductor (distributed parameter), while for the thermal–hydraulics of the helium coolant it includes a compressible 1D flow model. The AC losses induced by a pulsed coil in the NbTi poloidal field full size joint sample (PF-FSJS) right leg conductor, tested in 2002 at the Sultan facility in Villigen (CH), are considered as test bed for this exercise. The computed energy deposition and evolution of the temperature downstream of the heated zone are in good agreement with the measured values. However, the inter-bundle electrical conductances needed in input by the code are compatible with measured values only when a sufficiently refined model is used in the cable cross-section.

© 2005 Elsevier B.V. All rights reserved.

**Keywords:** ITER; NbTi; Superconducting coils; AC losses; Cable-in-conduit conductors; Numerical modeling

### 1. Introduction

The thermal–hydraulic electromagnetic (THELMA) code is a tool for the numerical simulation of the behavior of cable-in-conduit multi-strand superconductors (CICC), like those to be used for the magnets

of ITER [1]. The code solves simultaneously the electromagnetic and the thermal–hydraulic coupled problems. Its peculiarity, compared to other existing tools [2], is the principle capability to analyze long CICC lengths with complex geometry, electrically connected by means of resistive joints, as foreseen for the ITER coils.

The THELMA code is based on three different coupled modules: (1) a module for the joints and terminations analysis, based on a linear lumped electrical

\* Corresponding author. Tel.: +39 011 564 4490;  
fax: +39 011 564 4499.

*E-mail address:* [roberto.zanino@polito.it](mailto:roberto.zanino@polito.it) (R. Zanino).

circuit in transient or steady-state regime [3], (2) a module for the analysis of the current distribution in the different cable elements, implementing a non-linear distributed parameter model of the cable [4], and (3) a thermal–hydraulic module, for the thermal–hydraulic description of the solid and fluid components in a dual-channel CICC, typical for ITER conductors, mainly based on the model implemented in the Mithrandir code [5]. All the individual modules, as well as the coupling of a subset of them, have already been validated in the past [6–8].

In this paper, we present a first validation of the full version of the code, against data from the AC tests on the ITER NbTi poloidal field full size joint sample (PF-FSJS) [9], performed in 2002 at the SULTAN facility of PSI Villigen (CH) [10]. The AC losses are induced in the cable by the magnetic field generated by a pulsed coil. Four different AC loss tests are considered, with the external sinusoidal pulsed field frequency ranging from 2 to 5 Hz. All these shots have zero transport current, background magnetic field  $B_{DC} = 2$  T, current amplitude in the AC coil  $I_{AC} \sim 120$  A (leading to an AC field amplitude  $\sim 0.1$  T) and mass flow rate kept constant at  $\sim 4$  g/s.

## 2. Experimental set-up

The sample is made of two “legs” (=straight parallel vertical pieces of ITER-type CICC),  $\sim 3.5$  m long, made of different type of strands, both having petal wrappings (AISI 316L tapes, 0.1 mm thick, with  $\sim 88\%$  coverage), electrically connected in series at their bottom with a resistive joint [9]. The two legs are connected to the facility power supply through the upper terminations, see Fig. 1. Each leg is cooled with supercritical He at typically  $\sim 5$  K and  $\sim 1$  MPa in forced convection from the top to the bottom. A pulsed saddle coil applies a horizontal AC magnetic field (orthogonal to  $B_{DC}$ ), in the “plane” of the two legs, which induces the AC losses. The thermometers, and in particular those downstream of the pulsed field (heated) zone, can be used for the comparison with the simulations.

## 3. Model description

In THELMA, the PF-FSJS cable cross-section has been modeled comparing two different options:

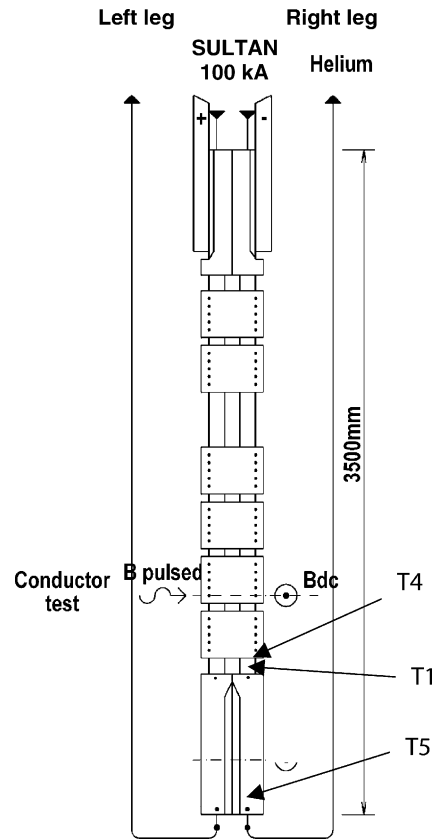


Fig. 1. Schematic view of the PF-FSJS sample. Reproduced from [9].

- 6 cable elements (CE), corresponding to the petals, i.e., the last but one cabling stage;
- 24 CE, where each petal is modeled in turn by 4 strand bundles.

The applicability of the (cheaper) 6 CE model is in principle subjected to the assumption that the inter-petal AC losses are dominant with respect to the intra-petal. This hypothesis is, however, somewhat in conflict with the presence of the petal wrappings, whose high resistance decreases the inter-petal current transfer in the cable. The 24 CE model permits the computation of the intra-petal currents, and their corresponding losses. The AC coil is modeled in detail and it is fed with a known sinusoidal impressed current. The magnetic coupling between this coil and the CE's is responsible for the presence of AC eddy currents and losses and also the magnetic coupling between the CE's is considered.

Only the right leg, where the highest losses were measured, is simulated, since the coupling between legs is weak.

For a given geometrical model of the leg, the major free parameters of the electromagnetic model are the values of the inter-CE distributed conductance  $G_C$ . This is an average value per unit length and takes into account both distributed and spot contacts between the CE's. In the case of the 6 CE model, a single value for neighboring petals is needed, while the 24 CE model needs different values for the intra- and inter-petal contacts. In the analyses,  $G_C$  has been adjusted for each model to best fit the losses measured in the pulse with the highest AC field frequency, and then kept frozen at all frequencies.

The set of equations solved by THELMA is made of a linear algebraic-differential system for the voltages (EM joint module) and for the currents in each CE (EM conductor module), coupled to an Euler-like PDE system (TH module). The conductor is discretized in finite elements, while the joint is modeled with a set of 2D networks at selected axial locations (the TH grid is a superposition of the two EM grids). The coupling between the EM modules is implicit (LU decomposition of the sparse matrix) and achieved internally by imposing the same currents at the boundary of the modeled regions. The set of TH equations is solved implicitly but the coupling between EM modules and TH module is explicit.

#### 4. Results and discussion

Table 1 reports the  $G_C$  needed by THELMA for the best fit at the highest AC frequency. For the model with 6 CE,  $G_C$  is out of the measured range [11], confirming that an exceedingly high conductance has to be assumed if the AC losses are represented in

Table 1

Inter-cable element distributed conductance (S/m)

$N_{\text{CE}}^a$	Type	Measured $G_C$ [11]	THELMA $G_C^b$
6	Inter-petal	$3.0 \times 10^4 / 5.0 \times 10^4$	$2.0 \times 10^6$
24	Inter-petal	$3.0 \times 10^4 / 5.0 \times 10^4$	$5.0 \times 10^4$
24	Inter-bundle	$5.0 \times 10^7 / 6.0 \times 10^7$	$3.5 \times 10^7$

<sup>a</sup> Number of cable elements in the THELMA model.

<sup>b</sup> Needed for best fit.

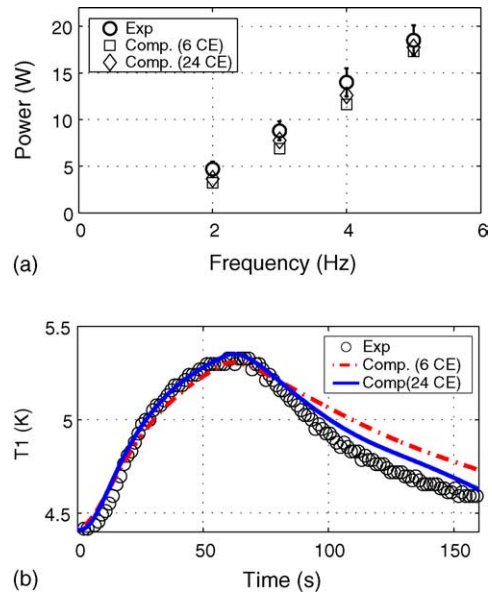


Fig. 2. (a) Comparison between measured (○) [12] and computed 6 CE (□) and computed 24 CE (◇), AC loss power as a function of the pulsed field frequency. (b) Comparison between measured (○) and computed 6 CE (---) and computed 24 CE (—) temperature evolution at T1 for the pulse at 5 Hz.

terms of inter-petal losses only. In the presence of petal wrappings, AC losses are generated mainly by the largest intra-petal current loops; therefore, a more refined model is needed for the cable geometrical description. This is confirmed by the results of the 24 CE model, which needs values of  $G_C$  which are very close to the measured range [11], both between CE's of the same petal and between neighboring petals.

The total power deposited in the cable is reported in Fig. 2a as a function of the pulse frequency. The temperature evolution at the T1 sensor (measuring the bundle helium temperature  $\sim 0.3$  m downstream of the pulsed field region) is reported in Fig. 2b, showing good agreement (within  $\sim 0.1$ – $0.2$  K) with the measured trace. Both models are able, with a single (albeit obviously different) set of  $G_C$ , to compute the deposited power with a good accuracy at all frequencies, within the experimental error bars. However, in the coarse (6 CE) model, local quantities like the induced current distribution, as well as the location of the dissipation, can be rather different from the actual ones, because of the ad-hoc nature of the  $G_C$ , while the refined model,

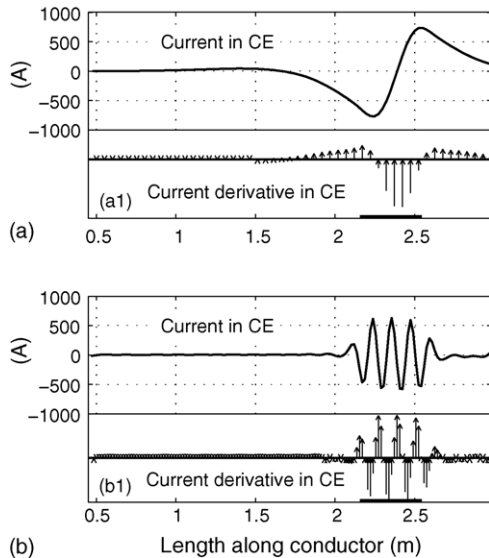


Fig. 3. Computed spatial profile along the conductor ( $x=0$  at the upper termination inlet) of the induced current in cable element “A”. (a) Case of 6 CE,  $A=1$  petal; (b) case of 24 CE,  $A=1/4$  petal. The arrows in (a1) and (b1) are proportional to  $dI/dx$ , giving an indication of the current transfer from and to cable element “A”. The location of the pulsed coil is also shown for reference (thick segment on the  $x$ -axis).

adopting a realistic  $G_C$  set, should give a more reliable simulation. For instance, one can compare Fig. 3a and b, showing that with the 6 CE model the total current transfer length results to be  $\sim 1.4$  m, which is larger than computed with the 24 CE model,  $\sim 0.6$  m. In each case, the computed length is roughly equal to the pulsed field length + one respective twist pitch ( $\sim 0.45$  m for the last but one stage and  $\sim 0.16$  m for the last but two stage, respectively), i.e., adding half a twist pitch on each side of the pulsed field region. With both models, only negligible current redistribution is present in the terminations.

## 5. Conclusions

A first validation of the full version of the THELMA code has been successfully performed on the AC-loss tests of the PF-FSJS. The results show that although different models of the cable cross-section (6 cable elements versus 24 cable elements) give both good results in terms of deposited power and temperature evolution,

only the more refined model uses, as best fit parameters, inter-cable element conductance values in a good agreement with laboratory measurements.

## Acknowledgment

The European Fusion Development Agreement (EFDA) partially financially supported this work.

## References

- [1] F. Bellina, T. Bonicelli, M. Breschi, M. Ciotti, A. Della Corte, A. Formisano, et al., Superconductive cables current distribution analysis, *Fusion Eng. Des.* 66–68 (2003) 1159–1163.
- [2] N. Mitchell, Modelling of non-uniform current diffusion coupled with thermohydraulic effects in superconducting cables, *Cryogenics* 40 (2000) 637–653; D. Ciazynski, J.-L. Duchateau, Validation of the CEA electrical network model for the ITER Coils, *IEEE Trans. Appl. Supercond.* 11 (2001) 1530–1533; A. Nijhuis, H.G. Knoopers, B. ten Haken, H.H.J. ten Kate, Model Study on AC loss and Current Distribution in a Superconducting Multi-Strand Cable, University of Twente Report UT-NET 2000-1, 2000; L. Bottura, C. Rosso, M. Breschi, A general model for thermal, hydraulic and electric analysis of superconducting cables, *Cryogenics* 40 (2000) 617–626.
- [3] F. Bellina, P. Bettini, F. Trevisan, Electromagnetic analysis of superconducting cables and joints in transient regime, *IEEE Trans. Appl. Supercond.* 14 (2004) 1356–1359.
- [4] M. Ciotti, A. Nijhuis, P.L. Ribani, L. Savoldi Richard, R. Zanino, Validation of the THELMA code against data from the ENEA stability experiment, *Cryogenics*, submitted for publication.
- [5] R. Zanino, S. De Palo, L. Bottura, A two-fluid code for the thermohydraulic transient analysis of CICC superconducting magnets, *J. Fusion Energy* 14 (1995) 25–40.
- [6] F. Bellina, D. Boso, B.A. Schrefler, G. Zavarise, Modelling a multistrand SC cable with an electrical DC lumped network, *IEEE Trans. Appl. Supercond.* 12 (2002) 1408–1412.
- [7] P.L. Ribani, CDCABLE: A Code to Calculate Current Distribution in Superconducting Multi-Filamentary Cables, University of Bologna Report, Task N. TW0-T400-1/101, May 2002.
- [8] R. Zanino, L. Bottura, C. Marinucci, Computer simulation of Quench propagation in QUELL, *Adv. Cryo. Eng.* 43 (1998) 181–188; R. Zanino, C. Marinucci, Heat slug propagation in QUELL. Part II: 2-fluid MITHRANDIR analysis, *Cryogenics* 39 (1999) 595–608; R. Zanino, P. Santagati, L. Savoldi, C. Marinucci, Joint+conductor thermal-hydraulic experiment and analysis on the Full Size Joint Sample using MITHRANDIR 2.1, *IEEE Trans. Appl. Supercond.* 10 (2000) 1110–1113.

- [9] P. Decool, D. Ciazynski, P. Libeyre, A. della Corte, M. Spadoni, S. Rossi, et al., Design and manufacture of a prototype NbTi full-size joint sample for the ITER poloidal field coils, *Fusion Eng. Des.* 66–68 (2003) 1165–1169.
- [10] D. Ciazynski, L. Zani, M. Ciotti, P. Gislou, M. Spadoni, S. Huber, et al., Test results on the first 50 kA NbTi full size sample for the International Thermonuclear Experimental Reactor, *Supercond. Sci. Technol.* 17 (2004) 155–160.
- [11] A. Nijhuis, Yu.A. Ilyin, W. Abbas, Electromagnetic and Mechanical Performance of Eight Prototype ITER NbTi Full-Size CICC's Under Transverse Loading up to 40,000 Cycles, University of Twente Report, 2004.
- [12] R. Zanino, P. Bruzzone, D. Ciazynski, M. Ciotti, P. Gislou, S. Nicollet, et al., Analysis of thermal–hydraulic gravity/buoyancy effects in the testing of the ITER poloidal field full size joint sample (PF-FSJS), *Adv. Cryo. Eng.* 49A (2004) 544–551.